



Assembled structures and magnetic properties of viologen-[M(mnt)₂] charge-transfer salts (mnt = maleonitriledithiolate; M = Cu, Ni, Pt)

Mochida, Tomoyuki
Funasakoa, Yusuke
Kishida, Takanori
Kachi-Terajima, Chihiro

(Citation)

Inorganica Chimica Acta, 384:111-116

(Issue Date)

2012-04-01

(Resource Type)

journal article

(Version)

Accepted Manuscript

(URL)

<https://hdl.handle.net/20.500.14094/90001811>



Assembled Structures and Magnetic Properties of Viologen–[M(mnt)₂] Charge-transfer Salts (mnt = maleonitriledithiolato; M = Cu, Ni, Pt)

Tomoyuki Mochida^{a,b,*}, Yusuke Funasako^a, Takanori Kishida^b, and Chihiro Kachi-Terajima^b

^a*Department of Chemistry, Graduate School of Science, Kobe University, Rokkodai, Nada, Hyogo 657-8501, Japan*

^b*Department of Chemistry, Faculty of Science, Toho University, Miyama, Funabashi, Chiba 274-8510, Japan*

Abstract

Ion-pair compounds of phenyl-substituted viologen dications with [M(mnt)₂] dianions were prepared and characterized. (Benzyl viologen)[M(mnt)₂] (M = Cu (**1**), Ni (**2**), Pt (**3**)) and (phenyl viologen)[Cu(mnt)₂] (**4**) exhibited mixed-stack crystal structures, whereas (dinitrophenyl viologen)[Cu(mnt)₂] (**5**) exhibited no π – π interactions. Magnetic susceptibility measurements revealed that **1** exhibits a ferromagnetic exchange interaction (Weiss constant $\theta = +0.9$ K), possibly mediated by the diamagnetic cation. Antiferromagnetic interactions were observed for **4** ($\theta = -2.0$ K) and **5** ($\theta = -2.9$ K), whereas **2** and **3** were diamagnetic. Absorption bands assignable to charge transfer were observed in the mixed-stack salts in the visible to near-infrared region.

Keywords: Magnetic properties / Charge transfer / Viologen / Metal dithiolenes / Copper

* Corresponding Author. Tel./fax: +81-78-803-5679

E-mail address: tmochida@platinum.kobe-u.ac.jp (T. Mochida)

1. Introduction

To date, a great deal of research has been carried out on charge-transfer (CT) complexes consisting of electron donors (D) and electron acceptors (A). Organic CT complexes with mixed-stack crystal structures usually become either neutral (D^0A^0) or ionic (D^+A^-), depending on the balance between the redox potentials of the components and the Madelung energy in the ionic state [1,2]. Similarly, molecules that afford stable monocations and dications, such as biferrocenes and viologens, produce monovalent ionic salts ($D^+A_n^-$) or divalent ionic salts ($D^{2+}A_n^{2-}$). Indeed, biferrocenium salts have been shown to exhibit transformation between the monovalent and divalent states by external stimuli [3]. Concerning viologens [4,5], many CT salts reported to date are predominantly divalent ion-pair compounds ($D^{2+}A_n^{2-}$) [5–8], although a few monovalent salts have also been reported [6b,9].

In this context, given our interest in the magnetism and valence states of viologen complexes, here we have prepared a series of CT salts using phenyl-substituted viologens and $[M(mnt)_2]$ anions (mnt = maleonitriledithiolate). Although many alkyl viologen complexes with metal dithiolates have been synthesized to date [6], their magnetic properties have not been thoroughly investigated. CT salts with $[M(mnt)_2]^{n-}$ are interesting from the viewpoint of magnetism, as they exhibit magnetic transitions and ferromagnetic interactions [10–12]. Among the anions, $[Cu(mnt)_2]^{2-}$ is a paramagnetic dianion that exhibits diverse coordination geometries around the copper atom, although there are relatively few examples of its complexes [13–15].

Herein we report the preparation, crystal structures, and magnetic properties of (benzyl viologen) $[M(mnt)_2]$ (M = Cu (**1**), Ni (**2**), Pt (**3**)), (phenyl viologen) $[Cu(mnt)_2]$ (**4**), and (dinitrophenyl viologen) $[Cu(mnt)_2]$ (**5**) (Figure 1). **1–4** exhibited mixed-stack crystal structures, whereas **5** showed no π - π stacking structure. **1**, **4**, and **5** were paramagnets. In particular, **1** exhibited a small ferromagnetic interaction, despite its mixed-stack structure with a diamagnetic cation.

2. Results and discussion

2.1. Syntheses

Single crystals of **1–5** were obtained by slow diffusion of solutions of the viologen dications in a

water-ethanol mixture and of $[M(\text{mnt})_2]$ dianions in acetone. These complexes were divalent solids with 1:1 stoichiometry ($D^{2+}A^{2-}$). In the infrared (IR) spectra, the CN stretching vibrations of the anions were observed at around 2180–2200 cm^{-1} , indicating that the acceptors are dianions [16]. A characteristic signal of Cu(II) [17] was consistently observed in the electron spin resonance (ESR) spectrum of **5**. The intramolecular bond lengths of the viologens and $[M(\text{mnt})_2]$ determined by crystallographic analyses (vide infra) are typical of those of viologen dications [6] and $[M(\text{mnt})_2]$ dianions [18], respectively.

2.2 Structures of Benzyl and Phenyl Viologen Salts **1–4**

1–3 were isomorphous, although **1** was slightly larger in cell volume than the other two [$V = 745.7 \text{ \AA}^3$ (**1**; $M = \text{Cu}$), 735.7 \AA^3 (**2**; $M = \text{Ni}$), and 736.5 \AA^3 (**3**; $M = \text{Pt}$) at 173 K; Table 1]. The packing diagram of **1** is shown in Fig. 2a. Both the viologens and $[M(\text{mnt})_2]$ are located on inversion centers, and half the molecules are crystallographically independent.

1–3 exhibit a mixed-stack structure ($\dots D^{2+}A^{2-}D^{2+}A^{2-} \dots$) along the b -axis (Fig. 2a). The bipyridinium moieties in the viologens are coplanar, and $[M(\text{mnt})_2]^{2-}$ dianions exhibit planar geometries. This contrasts with $[\text{H}_2\text{bpy}][\text{Cu}(\text{mnt})_2]$, in which non-planar cations and distorted anions are stacked alternately [15]. As seen in Fig. 2b, the cations and anions exhibit side-by-side co-planar arrangement along the $[1\ 1\ 0]$ direction, forming contacts between the pyridyl hydrogens and heteroatoms in $[M(\text{mnt})_2]$. A similar cation–anion arrangement is commonly seen in the structure of **4** (vide infra) as well as in (methyl viologen) $[M(\text{mnt})_2]$ ($M = \text{Ni}, \text{Pd}, \text{Pt}$ [6a,d]). The benzyl groups are located between the columns, having mutual π – π contacts. The centroid–centroid distance between the phenyl rings are 3.912 Å (**1**), 3.921 Å (**2**), and 3.981 Å (**3**).

The packing diagram of **4** is shown in Fig. 3. Both viologen and $[M(\text{mnt})_2]$ are located on inversion centers. The bipyridinium moiety in the cation is planar, and the terminal phenyl groups are tilted with respect to the bipyridinium moiety by 33° . This salt exhibits a mixed-stack structure, in which the stacking extends along $[110]$ for molecules on the (002) plane, and along $[1-10]$ for molecules on the (001) plane. Within the stacking columns, the molecular long axes of the viologen and $[\text{Cu}(\text{mnt})_2]$ are aligned in parallel, although their molecular planes are tilted with respect to each other by 7° . In addition, the molecular planes of the cations and anions are coplanar, arranged side-by-side as in **1–3**.

The stacking structures of **1** and **4** projected nearly along the molecular long axes are shown in Figs. 4a and 4b, respectively. In both structures, the intermolecular S...S distances ($> 4.41 \text{ \AA}$) are much longer than the vdW distance of 3.8 \AA , and there are no direct contacts between the anions. Significant intermolecular interactions exist only between the cation and anion through π - π stacking and side-by-side contacts. Hence, direct magnetic exchange between the anions should be negligible.

2.3 Structure of a Dinitrophenyl Viologen Salt **5**

The structure of **5** is much more complicated than those of **1-4**. In addition, it is exceptional in that it lacks a mixed-stack structure. The packing diagram is shown in Fig. 5. There are two pairs of crystallographically independent molecules in the crystal, denoted as D1, D2, A1, and A2. D1 and A1 are located on inversion centers, whereas D2 and A2 have no center of symmetry. Accordingly, the bipyridinium moiety is planar in D1, whereas the moiety is twisted by 32° in D2. The dinitrophenyl groups are twisted with respect to the pyridinium rings by 64° in D1 and by 80° and 83° in D2.

The cations and anions are arranged in a zigzag fashion with their long axes aligned in parallel (Fig. 5). The molecular planes of the bipyridinium moiety and the anion are highly twisted with respect to each other, and there is no direct π - π overlap between them. Although the nearest cation-anion pair is D1 and A2, their molecular planes are twisted relative to one another by 56° . Hence, CT interactions between D1 and A2 are expected to be small. The anions are surrounded by the dinitrophenyl groups and bipyridinium hydrogens of the cations. A2 forms a side-by-side centrosymmetric dimer-like arrangement, which has a long S...S intermolecular distance of 4.44 \AA .

2.4 Magnetic Susceptibilities

Magnetic susceptibility measurements revealed that **1**, **4**, and **5** were paramagnets, whereas **2** and **3** were diamagnetic. This is consistent with the valence states of the salts; $[\text{M}(\text{mnt})_2]^{2-}$ is paramagnetic for $\text{M} = \text{Cu}$ and diamagnetic for $\text{M} = \text{Ni}$ and Pt . The temperature dependence of the magnetic susceptibilities of the paramagnetic salts are shown in Fig. 6 in the form of χT versus T plots. The χT values at room temperature correspond to one spin per formula unit ($\chi T = 0.375 \text{ emu K mol}^{-1}$), which resides on the $[\text{Cu}(\text{mnt})_2]^{2-}$ anion.

The temperature dependence of the χT value obeyed the Curie–Weiss law, $\chi = C/(T-\theta)$. With decreasing temperature, the values for **1** increased at low temperatures, indicating the presence of a ferromagnetic interaction ($\theta = +0.89$ K). On the other hand, the values for **4** and **5** decreased, indicating antiferromagnetic interactions. The Weiss constants for **4** and **5** were $\theta = -2.04$ K and -2.92 K, respectively.

Considering the mixed-stack structure with the diamagnetic cation, the ferromagnetic interaction in **1** is noteworthy despite its small magnitude. In general, pyridinium salts with $[\text{Cu}(\text{mnt})_2]^{2-}$ exhibit antiferromagnetic interactions smaller than a few K [14a–c], although there is a salt that exhibits a slight ferromagnetic interaction ($\theta = +0.38$ K) [14d]. In **1**, the ferromagnetic exchange between $[\text{Cu}(\text{mnt})_2]^{2-}$ dianions may be communicated through the cation, giving rise to an intermolecular superexchange. Indeed, magnetic exchange mediated through non-magnetic counterions is suggested for $[\text{BDTA}]_2[\text{Cu}(\text{mnt})_2]$ ($J = -16$ K) [13] and $[\text{BDTA}][\text{Ni}(\text{mnt})_2]$ ($J = +2.20$ K) [19], as well as for a ferromagnet $[\text{NH}_4][\text{Ni}(\text{mnt})_2] \cdot \text{H}_2\text{O}$ [10a,b, 19] ($T_C = 4.5$ K). In **1**, however, a CT interaction is likely to exist between the cation and anion (vide infra), which might lead to an antiferromagnetic superexchange. Further studies, mainly theoretical, are needed to elucidate the interaction mechanism.

2.5 Solid-state Absorption Spectra

Ion-pair compounds between bipyridinium dications and metal-bis(dithiolene) dianions often exhibit CT absorption bands in the visible to near-IR region [6, 15]. The solid-state absorption spectra for **1–5** are shown in Fig. 7. Comparison of the spectra for **1–3** suggests that the intense broad bands at around 1.8 eV (~700 nm) as a shoulder in **1** and 1.5 eV (~850 nm) in **2** and **3**, not observed in their precursors, are assignable to the CT transition from $[\text{M}(\text{mnt})_2]^{2-}$ to $[\text{benzyl viologen}]^{2+}$. These are consistent with the redox potentials ($E^{2-/1-}$) of the anions [17b], 330 mV, 226 mV, and 210 mV (vs. SCE), for $M = \text{Cu}$, Ni , and Pt , respectively. The very weak absorption bands observable at around 1.1 eV (~1100 nm) in the copper complexes **1**, **4** and **5** may be d-d transitions in $[\text{Cu}(\text{mnt})_2]^{2-}$ [15], although the absorption in **5** is very slight. In **4**, a broad peak is observed at around 1.8 eV (~750 nm), which likely reflects the intramolecular transitions in phenyl viologen overlapped by a CT transition. No clear CT band was observed in **5**, consistent with the absence of π – π interactions between the cation and anion, as crystallographically demonstrated.

3. Conclusion

Ion-pair compounds of phenyl-substituted viologens with $[M(\text{mnt})_2]$ dianions were prepared. Salts with benzyl viologen and phenyl viologen exhibited mixed-stack crystal structures, whereas π - π interactions were absent in the salt with dinitrophenyl viologen. CT absorption bands were observed for the mixed-stack salts. Notably, a small but clear ferromagnetic interaction was found in (benzyl viologen) $[\text{Cu}(\text{mnt})_2]$. This is an interesting example of a ferromagnetic interaction that is mediated through diamagnetic molecules, as has previously been suggested only in a few other salts. Although many salts with viologens have been reported to date, magnetic investigations have been scarce. Our results suggest that ferromagnetic interactions may also be found in other viologen salts.

4. Experimental Section

4.1 Materials and physical measurements

Benzyl viologen dichloride (= 1,1'-dibenzyl-4,4'-bipyridinium dichloride), phenyl viologen dichloride (= 1,1'-diphenyl-4,4'-bipyridinium dichloride), dinitrophenyl viologen dichloride (= 1,1'-bis(2,4-dinitrophenyl)-4,4'-bipyridinium dichloride), and $(\text{NBu}_4)_2[\text{Ni}(\text{mnt})_2]$ were purchased from TCI. $(\text{NBu}_4)_2[M(\text{mnt})_2]$ ($M = \text{Cu}, \text{Pt}$) were prepared according to methods in the literature [20]. IR spectra were recorded as KBr pellets on a Thermo Nicolet Avatar 360 spectrometer. NIR-UV-vis absorption spectra of powder samples were recorded as KBr pellets on a JASCO V-570 UV/VIS/NIR spectrophotometer in a range of 250–2000 nm. Magnetic susceptibilities were measured under a magnetic field of 1 T in the temperature range of 2–300 K using a Quantum Design MPMS-XL SQUID magnetometer.

4.2 Preparation of Salts

Ion-pair compounds were prepared by diffusion methods. Typically, viologen dichloride (1.1×10^{-5} mol) and $(\text{NBu}_4)_2[M(\text{mnt})_2]$ (1.1×10^{-6} mol) were dissolved in 3 mL of a water-ethanol mixture (2:1 v/v) and acetone, respectively. These solutions, which were layered in a test tube and allowed to diffuse for a week, produced crystalline ion-pair compounds of **1–5**. Crystalline salts of (dinitrophenyl viologen) $[\text{Pt}(\text{mnt})_2]$ and

(benzyl viologen)[Ni(benzene-1,2-dithiolate)₂]₂ were also obtained but not structurally characterized because of their poor crystal quality.

4.2.1 (Benzyl viologen)[Cu(mnt)₂] (1)

Black needle crystals. FT-IR (cm⁻¹): 736, 742, 802, 825, 912, 1149, 1215, 1336, 1436, 1460, 1479, 1606, 1631, 2193 (CN), 2198 (CN), 3051, 3115 cm⁻¹. Anal. Calcd. for C₃₂H₂₂N₆S₄Cu (682.36): C, 56.32; H, 3.25; N, 12.32. Found: C, 56.14; H, 3.43; N, 12.14.

4.2.2 (Benzyl viologen)[Ni(mnt)₂] (2)

Brown needle crystals. FT-IR (cm⁻¹): 736, 742, 802, 825, 912, 1149, 1215, 1336, 1436, 1460, 1479, 1606, 1631, 2193 (CN), 2198 (CN), 3051, 3115 cm⁻¹. Anal. Calcd. for C₃₂H₂₂N₆S₄Ni (677.51): C, 56.73; H, 3.27; N, 12.40. Found: C, 56.53; H, 3.36; N, 12.17.

4.2.3 (Benzyl viologen)[Pt(mnt)₂] (3)

Black needle crystals. FT-IR (cm⁻¹): 736, 742, 802, 825, 912, 1149, 1215, 1336, 1436, 1460, 1479, 1606, 1631, 2193 (CN), 2198 (CN), 3051, 3115 cm⁻¹. Anal. Calcd. for C₃₂H₂₂N₆S₄Pt (813.92): C, 47.22; H, 2.72; N, 10.33. Found: C, 46.98; H, 2.88; N, 9.94.

4.2.4 (Phenyl viologen)[Cu(mnt)₂] (4)

Brown needle crystals. FT-IR (cm⁻¹): 759, 832, 913, 1150, 1431, 1485, 1629, 2195 (CN), 2215 (CN), 3037, 3114. Anal. Calcd. for C₃₀H₁₈N₆S₄Cu (654.31): C, 55.07; H, 2.77; N, 12.84. Found: C, 54.61; H, 2.96; N, 12.55.

4.2.5 (Ditrophenyl viologen)[Cu(mnt)₂] (5)

Black plate crystals. FT-IR (cm⁻¹): 736, 825, 912, 1149, 1336, 1436, 1460, 1541, 1606, 1631, 2193 (CN), 3051, 3115 cm⁻¹. Anal. Calcd. for C₃₀H₁₄N₁₀O₈S₄Cu (834.30): C, 43.18; H, 1.69; N, 16.79. Found: C, 42.94; H, 1.81; N, 16.39.

4.3 X-ray Structure Determination

Single crystal X-ray diffraction data were collected at 173 K on a Bruker SMART APEX II CCD diffractometer equipped with a graphite crystal and incident beam monochromator using Mo K α radiation (λ = 0.71073 Å). The structures were solved by the direct method (SHELXS 97 [21]) and expanded using Fourier techniques. The non-hydrogen atoms were refined anisotropically. The hydrogen atoms were placed at

idealized positions and allowed to ride on the relevant heavier atoms. Crystallographic parameters are listed in Table 1. ORTEP-3 [22] was used for molecular graphics.

CCDC 793659 (1), 793658 (2), 793657 (3), 795496 (4), and 793660 (5) contain the supplementary crystallographic data for this paper. These data can be obtained free of charge from The Cambridge Crystallographic Data Centre via www.ccdc.cam.ac.uk/data_request/cif.

Acknowledgements

We thank Dr. K. Mitsunaga (Toho University) for elemental analysis and T. Akasaka (Toho University) for his help with X-ray crystallography. This work was financially supported by a Grant-in-Aid for Scientific Research from Japan Society for the Promotion of Science (JSPS) and was carried out as part of the “High-Tech Research Center” Project (Toho University) 2005–2009 from the Ministry of Education, Culture, Sports, Science and Technology (MEXT), Japan. We thank M. Nakama (WarpStream Tokyo, Co., Ltd.) for providing a Web-based database system.

Appendix A. Supplementary material

CCDC 793659 (1), 793658 (2), 793657 (3), 795496 (4), and 793660 (5) contain the supplementary crystallographic data for this paper. These data can be obtained free of charge from The Cambridge Crystallographic Data Centre via www.ccdc.cam.ac.uk/data_request/cif.

References

- [1] G. Saito, Y. Yoshida, *Bull. Chem. Soc. Jpn.* 80 (2007) 1–137.
- [2] a) J.B. Torrance, J.E. Vazquez, J.J. Mayerle, V.Y. Lee, *Phys. Rev. Lett.* 46 (1981) 253–257; b) J.B. Torrance, A. Girlando, J.J. Mayerle, J.I. Crowley, V.Y. Lee, P. Batail, S.J. LaPlaca, *Phys. Rev. Lett.* 47 (1981) 1747–1750.
- [3] a) T. Mochida, K. Takazawa, M. Takahashi, M. Takeda, Y. Nishio, M. Sato, K. Kajita, H. Mori, M.M. Matsushita, T. Sugawara, *J. Phys. Soc. Jpn.* 74 (2005) 2214–2216; b) M. Uruichi, Y. Yue, K. Yakushi, T. Mochida, *J. Phys. Soc. Jpn.* 76 (2007) 124707/1–6.
- [4] S. Hünig, W. Schenk, *Liebigs Ann. Chem.* (1979) 1523–1533.
- [5] P.M.S. Monk, *The Viologens: physicochemical properties, synthesis and applications of the salts of 4,4'-bipyridine*, John Wiley & Sons, Chichester, 1998.
- [6] a) H. Kisch, *Com. Inorg. Chem.* 16 (1994) 113–132; b) H. Kisch, B. Eisen, R. Dinnebier, K. Shankland, W.I.F. David, F. Knoch, *Chem. Eur. J.* 7 (2001) 738–748; c) I. Nunn, B. Eisen, R. Benedix, H. Kisch, *Inorg. Chem.* 1994, 33, 5079–5085; d) M. Lemke, F. Knoch, H. Kisch, *Acta Cryst.* C49 (1993) 1630–1632.
- [7] a) G.J. Ashwell, *Phys. Stat. Sol.* b86 (1978) 705–715; b) G.J. Ashwell, S.C. Wallwork, *Acta Cryst.* B35 (1979) 1648–1651.
- [8] H. Kisch, A. Fernandez, Y. Wakatsuki, H. Yamazaki, *Z. Naturforsch.* 40b (1985) 292–297.
- [9] R. Benedix, M. Hofbauer, M. Möbius, F. Knoch, *Inorg. Chim. Acta* 262 (1997) 177–185.
- [10] a) N. Robertson, L. Cronin, *Coord. Chem. Rev.* 227 (2002) 93–127; b) C. Faulmann, P. Cassoux, *Prog. Inorg. Chem.*, 52 (2003) 399; c) C.L. Beswick, J.M. Schulman, E.I. Stiefel, *Prog. Inorg. Chem.* 52 (2003) 55, and references cited therein; d) S. Alvarez, R. Vicente, R. Hoffmann, *J. Am. Chem. Soc.* 107 (1985), 6253–6277; e) Z. Ni, X. Ren, J. Ma, J. Xie, C. Ni, Z. Chen, Q. Meng, *J. Am. Chem. Soc.* 127 (2005), 14330–14338.
- [11] a) T. Mochida, T. Koinuma, T. Akasaka, M. Sato, Y. Nishio, K. Kajita, H. Mori, *Chem. Eur. J.* 13 (2007) 1872–1881; b) T. Mochida, K. Takazawa, M. Takahashi, M. Takeda, Y. Nishio, M. Sato, K. Kajita, H. Mori, *Inorg. Chem.* 44 (2005) 8628–8641.
- [12] a) A.T. Coomber, D. Beljonne, R.H. Friend, J.L. Brédas, A. Charlton, N. Robertson, A.E. Underhill, M.

Kurmoo, P. Day, *Nature* 380 (1996) 144–146; b) M.L. Allan, A.T. Coomber, I.R. Marsden, J.H.F. Martens, R.H. Friend, A. Charlton, A.E. Underhill, *Synth. Met.* 56 (1993) 3317–3322; c) J. Nishijo, E. Ogura, J. Yamaura, A. Miyazaki, T. Enoki, T. Takano, Y. Kuwatani, M. Iyoda, *Solid State Commun.* 116 (2000) 661–664; d) M. Uruichi, K. Yakushi, Y. Yamashita, J. Qin, *J. Mat. Chem.* 8 (1998) 141–146; e) H. Nakajima, M. Katsuhara, M. Ashizawa, T. Kawamoto, T. Mori, *Inorg. Chem.* 43 (2004) 6075–6082; f) X. Ren, Y. Chen, C. He, S. Gao, *J. Chem. Soc., Dalton Trans.* (2002) 3915–3918.

[13] S.S. Staniland, W. Fujita, Y. Umezono, K. Awaga, P.J. Camp, S.J. Clark, N. Robertson, *Inorg. Chem.* 44 (2005) 546–551.

[14] a) X.M. Ren, J. Ma, C.S. Lu, S.Z. Yang, Q.J. Meng, P.H. Wu, *Dalton Trans.* (2003) 1345; b) Q. Huang, W.Q. Chen, X. Chen, X.B. Liu, J.R. Zhou, H.R. Zuo, L.L. Yu, C.L. Ni, *Trans. Met. Chem.* 34 (2009) 765–771; c) X.M. Ren, Z.P. Ni, S. Noro, T. Akutagawa, S. Nishihara, T. Nakamura, Y.X. Sui, Y. Song, *Cryst. Growth Des.* 6 (2006) 2530–2537; d) Q. Huang, J.H. Lin, L.B. Liang, X. Chen, H.R. Zuo, J.R. Zhou, L.M. Yang, C.L. Ni, X.L. Hu, *Inorg. Chim. Acta* 363 (2010) 2546–2552.

[15] V. Madhu, S.K. Das, *Polyhedron* 23 (2004) 1235–1242.

[16] S.P. Best, S.A. Ciniawsky, R.J.H. Clark, R.C.S. Mcqueen, *J. Chem. Soc., Dalton Trans.* (1993) 2267–2271.

[17] a) A.H. Maki, N. Edelstein, A. Davidson, R.H. Holm, *J. Am. Chem. Soc.* 86 (1964) 4580–4587; b) A. Davison, N. Edelstein, R.H. Holm, A.H. Maki, *Inorg. Chem.* 2 (1963) 1227–1232.

[18] D. Bellamy, A. Christofides, N.G. Connelly, G.R. Lewis, A.G. Orpen, P. Thornton, *J. Chem. Soc., Dalton Trans.* (2000) 4038–4043.

[19] Y. Umezono, W. Fujita, K. Awaga, *Chem. Phys. Lett.* 409 (2005) 139–143.

[20] R.H. Holm, A. Davison, *Inorg. Synth.* 10 (1967) 8.

[21] G.M. Sheldrick, *SHELXL: Program for the Solution for Crystal Structures*, University of Göttingen, Germany, 1997.

[22] L.J. Farrugia, *ORTEP-3 for Windows*, *J. Appl. Cryst.* 30 (1997) 565–566.

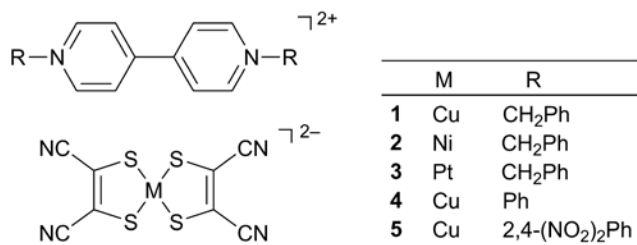


Fig. 1. Chemical formulas of **1**–**5**.

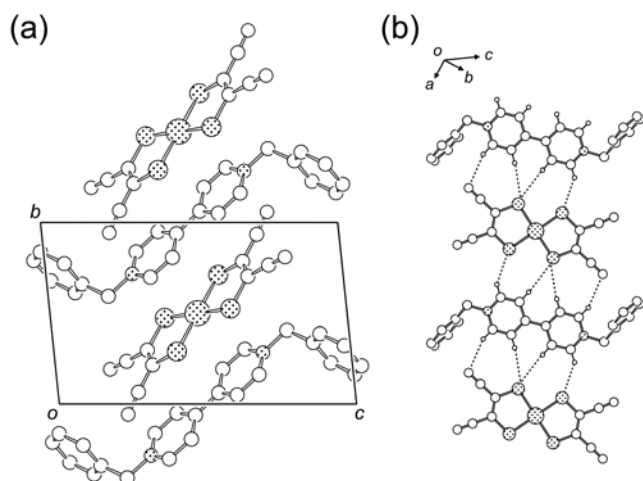


Fig. 2. (a) Packing diagram of **1** projected along the *a*-axis. Hydrogen atoms are omitted for clarity. (b) Molecular arrangements viewed perpendicular to the molecular planes. Dashed lines represent cation-anion contacts.

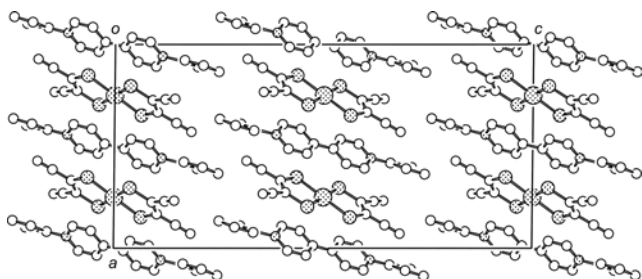


Fig. 3. Packing diagram of **4** viewed along the *a*-axis. Hydrogen atoms are omitted for clarity.

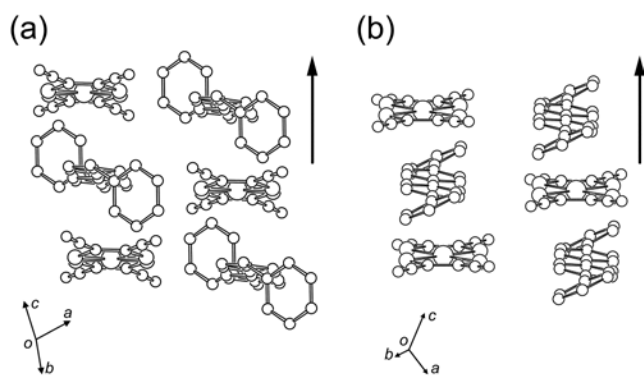


Fig. 4. Molecular arrangements in (a) **1** and (b) **4**, viewed nearly along the molecular long axes. The π - π stacking direction is shown by an arrow. Hydrogen atoms are omitted for clarity.

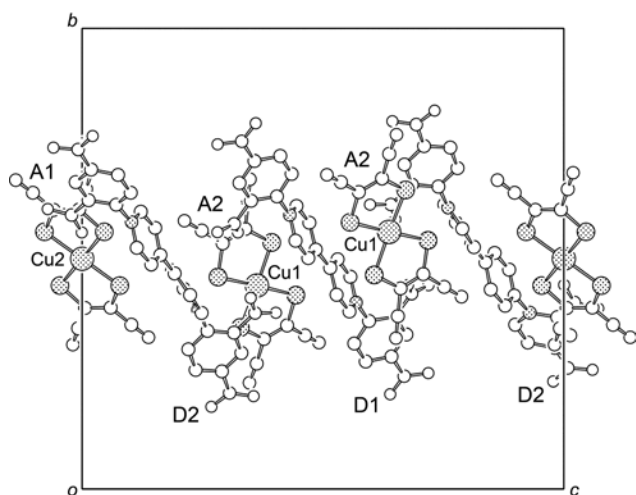


Fig. 5. Packing diagram of **5** viewed along the *b*-axis. Molecules on the *ac* planes are omitted. Hydrogen atoms are omitted for clarity.

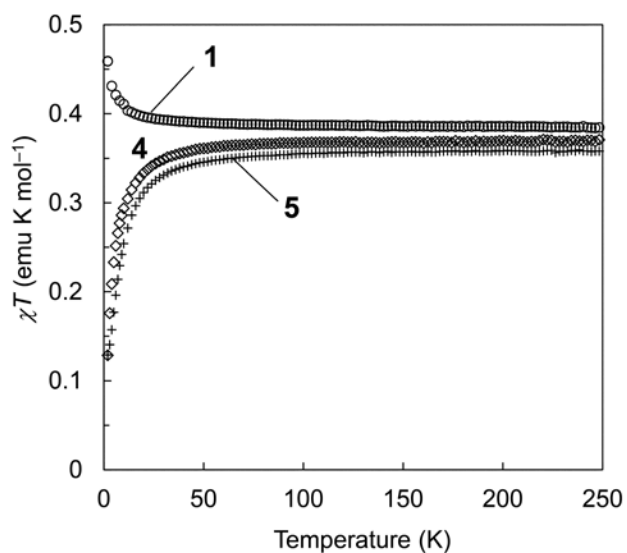


Fig. 6. Temperature dependence of magnetic susceptibilities of **1** (\circ), **4** (\diamond), and **5** ($+$), represented in the form $\chi_m T$ versus T .

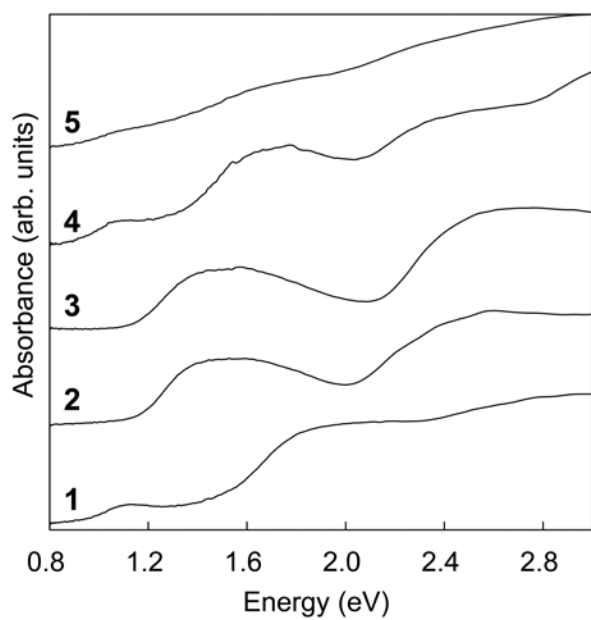


Fig. 7. Solid-state electronic spectra of **1–5**.

Table 1
Crystallographic Parameters

	1	2	3	4	5
Empirical formula	C ₃₂ H ₂₂ N ₆ CuS ₄	C ₃₀ H ₂₂ N ₆ NiS ₄	C ₃₂ H ₂₂ N ₆ PtS ₄	C ₃₀ H ₁₈ N ₆ CuS ₄	C ₃₀ H ₁₄ N ₁₀ CuO ₈ S ₄
Formula weight	682.34	677.51	813.92	654.28	834.48
Crystal size (mm ³)	0.38×0.15×0.03	0.15×0.08×0.05	0.30×0.25×0.03	0.61×0.14×0.02	0.5×0.13×0.03
Crystal system	Triclinic	Triclinic	Triclinic	Monoclinic	Monoclinic
<i>a</i> (Å)	6.6279(6)	6.5384(11)	6.4844(6)	13.391(4)	9.3198(7)
<i>b</i> (Å)	8.9564(8)	8.9767(19)	9.0975(9)	7.542(2)	22.5924(16)
<i>c</i> (Å)	13.5994(12)	13.536(2)	13.4236(13)	27.630(7)	23.7992(17)
α (deg)	95.555(2)	83.376(5)	94.424(2)		
β (deg)	90.727(2)	88.017(3)	93.233(2)	90.634(4)	90.6920(10)
γ (deg)	111.6750(10)	68.794(3)	110.517(2)		
<i>V</i> (Å ³)	745.66(12)	735.7(2)	736.48(12)	2790.4(13)	5010.7(6)
Space group	<i>P</i> -1	<i>P</i> -1	<i>P</i> -1	<i>C</i> 2/ <i>c</i>	<i>P</i> 2 ₁ / <i>c</i>
<i>Z</i> value	1	1	1	4	6
<i>D</i> _{calc}	1.52	1.529	1.835	1.557	1.643
<i>F</i> (000)	349	348	398	1332	2105
No. of reflections	4753	4687	5012	7464	31439
No. of observations	3412	3328	3591	3101	11464
Parameters	197	196	196	187	718
Temperature (K)	173	173	173	173	173
<i>R</i> ₁ ^a , <i>wR</i> ₂ ^b (<i>I</i> > 2σ(<i>I</i>))	0.0470, 0.1266	0.0767, 0.1283	0.0353, 0.0747	0.0356, 0.0835	0.0476, 0.0832
<i>R</i> ₁ ^a , <i>wR</i> ₂ ^b (all data)	0.0695, 0.1473	0.1359, 0.1464	0.0363, 0.0752	0.0467, 0.0893	0.1211, 0.1043
Goodness-of-fit	1.026	1.046	0.975	1.028	0.953

$$^a R_1 = \sum ||F_o| - |F_c|| / \sum |F_o|.$$

$$^b wR_2 = [\sum w(F_o^2 - F_c^2)^2 / \sum w(F_o^2)^2]^{1/2}.$$

TOC

